The 532 nm Laser Treatment Promotes The Proliferation of Tendon-Derived Stem Cells and Up-Regulates Nr4a1 To Stimulate Tenogenic Differentiation

Ming Li
Shanghai 9th Peoples Hospital Affiliated to Shanghai Jiaotong University School of Medicine Department of Plastic Surgery https://orcid.org/0000-0003-2663-598X

Yiming Zhu
Shanghai Jiao Tong University School of Medicine Affiliated Ninth People's Hospital

Qing Pei
Shanghai 9th Peoples Hospital Affiliated to Shanghai Jiaotong University School of Medicine Department of Plastic Surgery

Yuhao Deng
Shanghai 6th Peoples Hospital Affiliated to Shanghai Jiaotong University

Tao Ni (nitao8888@yeah.net)
Shanghai Jiao Tong University

Research

Keywords: LLLT, tendon repairing, TDSCs, tenogenic differentiation, Nr4a1

Posted Date: October 12th, 2021

DOI: https://doi.org/10.21203/rs.3.rs-960303/v1

Abstract

Background

The combination of low-level laser therapy (LLLT) and stem cell transplantation with tendon-derived stem cells (TDSCs) as seed cells provides a new treatment strategy for tendon injury. Nevertheless, the effect of LLLT on the biological behavior of TDSCs and its internal mechanisms remain unclear. The purpose of this study was to verify the effect of LLLT with a wavelength of 532 nm on the proliferation and differentiation of TDSCs of Sprague-Dawley (SD) rats.

Methods

TDSCs were isolated from Achilles tendons of SD rats and identified by cell morphology and flow cytometric analysis. Energy density gradient experiment was performed to determine the ideal energy. Then TDSCs were treated with LLLT using a wavelength of 532 nm at a fluence of 15J/cm^2. Cell response after irradiation was observed at 6, 12 and 24 hours to ascertain cell morphology and cell proliferation. RT-PCR was used to detect the RNA expression levels of the key genes of TDSCs differentiation including *Scx*, *Tnmd*, Mkx and *Dcn*, *PPARγ*, *Sox9* and *Runx2*. Then gene chip microarray was used to detect the expression of differential genes after 532 nm laser intervention in TDSCs, and the target genes were screened out to verify the role of target genes in this process.

Results

When the 532 nm laser energy density was 15 J/cm^2, the proliferation capacity of TDSCs was improved (2.73 ± 0.24 vs. 1.81 ± 0.71, $P < 0.05$), and the expression of genes related to tenogenic differentiation of TDSCs was significantly increased ($P < 0.01$), showing the potential of tenogenic differentiation. After RNA-seq and bioinformatics analyses, we speculated that Nr4a1 was involved in the tenogenic differentiation process of TDSCs regulated by 532 nm laser treatment. Subsequent experiments confirmed that Nr4a1 regulated the expression of the tenogenic differentiation genes scleraxis (*Scx*) and tenomodulin (*Tnmd*) in TDSCs, affecting the process.

Conclusion

A 532 nm laser with 15J/cm^2 regulated the process of TDSC proliferation and tenogenic differentiation by up-regulating Nr4a, which could accelerate tendon healing.

Background

With population aging and the promotion of sports, the number of people suffering from tendon injuries is growing, with such injuries affecting younger and younger populations. According to the epidemiological statistics, approximately 45% of musculoskeletal injuries are tendon or ligament injuries in the US, and the incidence of tendon injury is more than 40% in baseball players and long-distance runners [1]. Surgical treatment, which is the main treatment method for tendon injury, mainly involves the combination of tendon suture and external fixation [2]. However, problems remain concerning postoperative tendon mechanical strength, scar tissue hyperplasia, tissue adhesion, etc. [3]. Therefore, identifying a tendon repair strategy with less damage and high efficiency is of urgent importance.

Over recent years, stem cell transplantation in tissue engineering has become widely used to treat tendon injury. Mesenchymal stem cells (MSCs), which have a wide range of sources, are relatively simple to obtain. These cells also have the potential for rapid proliferation and multidirectional differentiation under specific conditions, and are thus important seed cells for tissue engineering [4]. For example, adipose-derived stem cells (ADSCs) have been applied in tendon repair [5]. Tendon-derived stem cells (TDSCs) not only have the characteristics of mesenchymal stem cells, comparable to the more commonly-used seed cells such as bone marrow stem cells (BMSCs), but can also highly express tendon-related genes and proteins, such as scleraxis (*Scx*), tenomodulin (*Tnmd*), and mucin C, and have a special tendency to differentiate into tendon cells [6, 7]. Therefore, numerous researchers have explored the application of TDSCs in the treatment of injured tendons [8]. Some researchers transplanted TDSCs into a rat model of patella tendon injury and found that, compared with the control group, the repaired tendon showed a more orderly arrangement of fibrous tissue and stronger biomechanics after 8 weeks [9]. Still, there are some practical problems in applying stem cells in clinical treatment, such as unclear differentiation mechanism, maintenance of the differentiation ability of stem cells, and difficulty in controlling the direction of differentiation [6].

Low level laser therapy (LLLT) is a non-invasive phototherapy method that uses a laser to biologically stimulate cells without thermal stimulation, affecting the biological behavior of cells and accelerating tissue repair and reconstruction [10]. Since the discovery of lasers in the 1960s, LLLT has shown great prospects for clinical application, such as in wound healing, androgenetic alopecia, muscle pain relief, and regulation of inflammation, because of its advantages of causing only slight damage, its strong operability, and nontoxic side effects [11, 12]. Studies have shown that LLLT can regulate the proliferation and differentiation of MSCs. Tani *et al.* reported that a 635 nm laser regulates differentiation of BMSCs into osteoblasts by activating the AKT signaling pathway, which enhances cytoskeletal construction and bone mineralization formation patterns [13]. The effects of LLLT of different wavelengths and energy densities on MSCs are different. In a study comparing the effects of a 630 nm laser and an 810 nm laser on the proliferation of ADSCs at energy densities of 0.6 J/cm^2, 1.2 J/cm^{2,} and 2.4 J/cm^2, it was found that a 630 nm laser with energy density of 1.2 J/cm^2 and an 810 nm laser of 2.4 J/cm^2 had the strongest effect on the activity of ADSCs [14]. Numerous studies have shown that LLLT at a specific wavelength and appropriate energy density activated MSCs and promote their proliferation and differentiation *in vitro*.

Our research group is devoted to exploring the mechanism of a 532 nm laser and its effect on tendon repair. In our previous study, we used an optical treatment method called photochemical tissue bonding (PTB) which employed a 532 nm laser and the photosensitizer Rose Bengal (RB) to treat Achilles tendon injury in rats. Our results revealed that such an approach promoted repair of the injured tendon, and the biomechanical strength of the tendon was also significantly enhanced. Furthermore, study of the mechanism revealed that the continuous low release level of reactive oxygen (ROS) in tendon cells treated with a 532 nm laser activates the RhoA/NF-κB pathway, thereby promoting the proliferation and migration of tendon cells and accelerating tendon healing [15, 16]. Most researchers believe that TDSCs have an important role in repairing injured tendon [17, 18]. Whether the proliferation and differentiation of TDSCs can be regulated to promote the repair of the injured tendon during the process of 532 nm laser-induced repair of injured Achilles tendon remains to be elucidated.

Accordingly, the current study aimed to isolate, identify, and culture TDSCs from SD rats. Additionally, after identifying a reasonable energy density of TDSCs irradiated by a 532 nm laser, the influence of the 532 nm laser on the proliferation and differentiation of TDSCs was investigated. RNA sequencing (RNA-seq) was used to detect differentially-expressed genes in TDSCs after 532 nm laser irradiation, and the key genes were screened and verified by bioinformatics analysis so as to explore the possible mechanism via which the 532 nm laser regulated the proliferation and differentiation of TDSCs.

Materials And Methods

TDSC isolation and cell culture

Achilles tendons (AT) were harvested from one of the hindlimbs of Sprague–Dawley (SD) rats, anesthetized with 0.5% pentobarbital sodium (0.3 mL/100 g, Sigma-Aldrich) by intraperitoneal administration. Pieces of the ATs 0.5 × 1.0 cm^2 were isolated, cut into 0.25 cm^3 pieces and digested with type I collagenase (2 mg/mL; Sigma-Aldrich, St Louis, MO, USA) in DMEM supplemented with 2% fetal bovine serum for 16 h at 37°C and collected using a 70-mm cell strainer to produce a single cell suspension. The cells were washed in PBS by centrifugation at 800 × *g* for 5 min then reseeded at 1 × 10^4 cells/cm^2 in monolayer cultures in complete high glucose DMEM (HG-DMEM) supplemented with 20% fetal bovine serum, 100 U/mL penicillin, and 100 mg/mL streptomycin. After 24 h of initial culture, the rapidly-adherent, fibroblast-like cells were excluded by transferring the nonadherent cells to fresh culture flasks. At day 7, TDSCs were trypsinized and mixed together as passage 0, after which they were passaged four or five times before use for experiments.

Flow cytometry assay

In order to confirm the presence of surface antigens characteristic of TDSCs, TDSCs at passage 4 were harvested by digestion with 0.25% trypsin/ ethylenediaminetetraacetic acid (EDTA) as described above. Approximately 1 × 10^6 cells separated through centrifugation were incubated with 1 mg fluorescein isothiocyanate (FITC) or phycoerythrin (PE) fluorescent dyes conjugated with anti-rat monoclonal

antibodies (CD44, CD45, and CD90), then fixed in 4% paraformaldehyde at room temperature for 20 minutes. After washing with 200 μL PBS (pH = 7.4), cells were removed from the fixing solution and resuspended in PBS for flow cytometry. Analysis of the phenotypic results was performed with an FC 500 Flow Cytometry Analyzer (Beckman Coulter, Brea, CA, USA).

Laser intervention method

A 532 nm Nd:YAG laser (Oculight; Iridex, Mountain View, CA, USA) with a diameter of 5 mm was used. During the irradiation, the distance between the laser emitter and the cell layer was kept at 6 cm for all cell groups. Sterile foil was used to create an enclosed space to prevent interference caused by light dispersion and refraction. After irradiation, the cells were returned to the incubator for further culture, and the stem cell culture medium was replaced every 1–2 days.

Cell Titer-Glo (CTG) assay

In order to determine the effect of 532 nm laser irradiation with different energy densities on cell viability, so as to choose a reasonable energy density for subsequent experiments, cells were seeded into 96-well plates at a density of 1×10^4 cells/well. The cells were then assigned to one of seven energy density laser groups (0 J/cm^2, 1.5 J/cm^2, 3 J/cm^2, 6 J/cm^2, 9 J/cm^2, 15 J/cm^2 and 24 J/cm^2). The irradiation times for these seven groups were: 0 s, 30 s, 60 s, 2 min, 3 min, 5 min, and 8 min, respectively. The CTG assay was performed at 24 and 48 h after a single exposure.

Crystal Violet assay

To determine the effects of 532 nm laser irradiation on cell activity and proliferation, cells were seeded into 96-well plates at a density of 1×10^4 and incubated at 37°C in a constant temperature incubator. After 6, 12, or 24 h, the culture medium was removed, and cells were fixed with 4% paraformaldehyde (PFA) solution for 15 min at room temperature (RT). Then, cells were washed with PBS, and each well was stained with 100 μL of 0.2% Crystal Violet solution in PBS for 15 min at RT. Deionized water was used to wash the dye solution from the plates, and the dye was then solubilized in 100 μL of 1% sodium dodecyl sulfate (SDS) solution in PBS. Optical density (OD) was measured at an emission wavelength of 570 nm using a microplate reader to compare the cell proliferation of the two groups.

Quantitative real-time reverse transcription-polymerase chain reaction (RT-PCR)

RT-PCR was performed to analyze the differentiation-related gene expression after 24 and 48 h of 532 nm laser single irradiation. Total RNA was extracted using an RNA purification kit (Corning, Corning, NY, USA) according to the manufacturer's instructions. Reverse transcription (RT) was performed using a Prime Script RT Reagent Kit (Takara Bio Inc., Shiga, Japan) to reverse transcribe RNA into cDNA. Real-time PCR was quantified using SYBR Premix Ex Taq (Takara Bio Inc.) in a Light Cycler® 96 System (Roche, Basel, Switzerland). The specific primers for differentiation-related genes (Invitrogen, Carlsbad, CA, USA) used in this study are listed in **Table 1**. GAPDH was used as an internal control. The results are presented as the

relative expression ratios of the target sample to the control group for each sample, calculated using the $2^{-\Delta\Delta CT}$ method.

Western blotting

Total protein was collected from cultured cells using Lysis Buffer (RIPA, Beyotime, Shanghai, China) supplemented with 1% protease inhibitor (Roche Applied Science), and a total of 40 μg protein were loaded for electrophoresis. The proteins were separated by SDS polyacrylamide gel electrophoresis (SDS-PAGE) using a 10% gel, and transferred to a nitrocellulose membrane (Merck Millipore, Darmstadt, Germany). Membranes were blocked for 1 h with 5% nonfat milk at RT, and blots were probed with the following antibodies: anti-Nr4a1 (1:1,000, ab13851, Abcam, Cambridge, UK), anti-Scx (1:1,000, ab185940, Abcam), and anti-tenomodulin (1:1,000, ab203676, Abcam) at 4°C overnight. After washing in Tris-buffered saline containing Tween, the membrane was incubated with anti-rabbit IgG (1:1,000, ab205718, Abcam) for 1h at RT.

Gene chip microarray assay and analysis

After 48h of 532 nm single laser irradiation, cells of 532 nm laser group and control unirradiated cells were dissolved in Trizol (Life Technologies, USA) for total RNA isolation. RNA concentration was quantified using the EXON Gene Chip instrument (Affymetrix, Thermo Fisher Scientific, Waltham, MA, USA), and RNA integrity was assessed using an Agilent Bioanalyzer 2100 (Agilent Technologies, Santa Clara, CA, USA). For gene expression analysis, the Gene Chip Command Console software version 4.0 (Affymetrix) was used to extract raw data according to the manufacturer's instructions. Basic analysis was performed using the Gene software version 13.1 (Agilent Technologies). RNA normalization was performed using the Expression Console software version 1.3.1 (Affymetrix). Ultimately, Kyoto Encyclopedia of Genes and Genomes (KEGG) pathway and gene ontology (GO) analyses were applied to clarify the molecular functions of up-regulated genes and relevant pathways.

Tendon injury model

Thirty-six SD rats (male, 6-weeks-old) were obtained from the Laboratory Animal Services Centre. All the animals were housed in an environment with a temperature of 25 ± 1ºC, a relative humidity of 65 ± 5%, and a light/dark cycle of 12/12 hr. Animals were given water and sterilized food *ad libitum*. All animal studies (including the rat euthanasia procedure) were carried out in compliance with the regulations and guidelines of Shanghai Jiao Tong University institutional animal care and conducted according to the AAALAC and the IACUC guidelines.

Thirty-six rats were divided into two groups: a control group and a 532 nm laser group. For the tendon injury model, we adopted a rat model of Achilles-tendon injury following a previously-reported method [19]. The Achilles tendon was separated from the plantaris and soleus tendons and injury were surgically induced by semi-cutting, followed by primary suture repair. For rats in the laser group, the tendon was

irradiated with a 532 nm laser and then sutured, while for those in the control group the tendons were directly sutured. Tendon tissue samples were collected 7 days after modeling.

Hematoxylin and eosin (H&E) staining

Normal and degenerative tendons were fixed with 4% paraformaldehyde, dehydrated with 30% sucrose, embedded in OCT (Sakura Finetek, Torrence, CA, USA), and frozen at -80°C before sectioning. Cryosections were cut at 5 μm thickness and stained with H&E (Sakura Finetek) to observe cell morphology and cell number. The samples were imaged using an upright microscope (Olympus, Tokyo, Japan).

Immunohistochemistry

The specimens of the tendon injury model were collected and divided into two groups for histological tests. The tissues were fixed in 4% paraformaldehyde solution, dehydrated with a series of graded ethanol, and then embedded in paraffin. Sections were stained as 5 mm-thick sections with Anti-Nr4a1 (1:1,000, ab13851, Abcam). After nonspecific reactive sites were blocked with 5% bovine serum albumin, slides were incubated overnight at 4°C with anti-rat targeted antibodies at 1:200 to 1:500 dilutions and then conjugated with goat anti-rabbit IgG (1:1500; Santa Cruz Biotechnology, Santa Cruz, CA, USA) secondary antibody in the dark at RT for 1 h. Finally, the sections were stained with 3,3'-diaminobenzidine and then counterstained with hematoxylin.

Cell transfection

The Nr4a1 coding sequence was cloned into the pCDNA3.1 (+) vector. The primers were as follows:

F: ATGCGATTCTGCAGCTCTTCC,

R: GGGTGGTATTGTCGTAGTAGAAGG.

TDSCs (5×10^3 cells/well) were plated into 6-well plates and transfected with either blank pCDNA3.1 (+) vector or pCDNA3.1(+)-Nr4a1. The transfection was performed using Lipofectamine 2000 reagent (Invitrogen) according to the manufacturer's instructions. After 6–8 h, TDSCs were washed and cultured for 24 h in complete medium.

Statistical analysis

All individual experiments were performed at least three times, with three replicates. Data are expressed as means ± standard deviation (SD). All statistical analyses were carried out using SPSS 13.0 (IBM, Armonk, NY, USA). Differences among more than two experimental groups were evaluated by one-way ANOVA. $P \leq 0.05$ was considered statistically significant. Image J and GraphPad Prism software were used for plotting calculations.

Results

Isolation and characterization of TDSCs

Cells were isolated from Achilles tendons of SD rats and formed initial colonies when inoculated into culture dishes at low density. The cell morphology was cobblestone-like, and the cells had clone-forming ability after subculture (Fig. 1a), which was in accordance with other reports [20]. In addition, the separated cells exhibited homogeneous spindle-shaped or fibroblastic features, and the morphology remained stable for several passages (Fig. 1b). Furthermore, when compared with isotype control by flow cytometric analysis, 95.3% of cells were positive for CD44 (Fig. 1c), and 97.6% were positive for CD90 (Fig. 1e), but they were negative for the leukemia cell marker CD45 (Fig. 1d). These data demonstrated that the isolated cells had characteristics of stem cells indicating that they were TDSCs.

3.2 The energy density gradient experiment of TDSCs was regulated by the 532 nm laser.

The CTG fluorescent cell viability test is a method that indirectly reflects cell viability by measuring the synthesis of adenine nucleoside triphosphate (ATP) in cells. We used CTG to measure the OD value of TDSCs at 12 and 24 h after a single 532 nm laser irradiation. The experimental results (Fig. 2) revealed that when the energy density of the 532 nm laser exceeded 6 J/cm^2, the cell activity of TDSCs in each group significantly increased compared with that in the control group ($P < 0.01$), and the cell activity of TDSCs also increased with the increase of energy density. However, when an energy density of 15 J/cm^2 or 24 J/cm^2 was used, there was no significant difference in the cell viability of TDSCs in the two groups ($P > 0.05$). Therefore, we selected the 15 J/cm^2 group for subsequent study.

The 532 nm laser stimulated the proliferation of TDSCs.

To investigate the impact of the 15 J/cm^2 532 nm laser on the proliferative ability of TDSCs, we used the Crystal Violet staining method to analyze the number of cells in the control group and the 532 nm laser-treated group at 6, 12, and 24 h (Fig. 3a). When the cells were cultured for 6 h, the TDSCs of the two groups were adherent to the wall, and the cell inoculation density was basically the same. At 24 h, the cell morphology was polygonal, and the number of cells in the 532 nm laser group significantly increased. After dissolving the Crystal Violet with SDS, the OD values of the two groups were measured (Fig. 3b). This showed that the OD value of the 532 nm laser group was significantly higher than the control group (2.73 ± 0.24 vs.1.81 ± 0.71, $^*P < 0.05$). Thus the 532 nm laser at 15 J/cm^2 can promoted the proliferation of TDSCs.

Irradiation with a 532 nm laser regulated the differentiation of TDSCs.

To investigate the effect of 532 nm laser irradiation on the differentiation ability of TDSCs, RT-PCR was used to analyze the RNA expression levels of the key genes of TDSC differentiation, *Scx*, *Tnmd*, *Mkx*, and *Dcn* (related to tendinous differentiation), *PPARγ* (adipogenic marker gene), *Sox9* (chondrogenic marker gene) and *Runx2* (osteogenic marker gene). Our data showed that at 24 and 48 h, the expression levels of

Scx and *Tnmd* genes in TDSCs in the 532 nm laser group were significantly increased compared with those in the control group, showing a statistically-significant difference ($^{**}P < 0.01$). In contrast, the markers of adipogenic, chondrogenic, and osteogenic differentiation did not significantly change ($P > 0.05$), which indicated that after 532 nm laser intervention, the tenogenic differentiation-related markers of TDSCs were highly expressed, inducing the cells to differentiate into tendon cells.

The Nr4a1 and the TGF-β signaling pathway is involved in the process of TDSC differentiation regulated by 532 nm laser irradiation.

To investigate the mechanism of 532 nm laser irradiation in regulating the differentiation process of TDSCs, gene expression was analyzed in TDSCs collected from the laser-treated group and the control group using gene chip microarray (Fig. 5a). GO and KEGG pathway analyses were performed to confirm the roles of up-regulated genes in molecular functions and pathways. Skeletal muscle tissue development and skeletal muscle cell differentiation were both enriched in the biological process category of GO analyses (Fig. 5b). In addition, the TGF-β signaling pathway was enriched in KEGG pathway analysis of up-regulated genes (Fig. 5c).

Among the 795 differentially-expressed genes identified by gene chip microarray, 15 genes that were closely related to the signaling pathways enriched by GO analysis and KEGG pathway analysis included *Nr4a1*, *Tnmd*, *Scx*, *Fos*, *Egr1*, and *Btg2*. These genes related to the TGF-β pathway showed a significant difference in expression between the two groups. According to the literature review, among these genes, Nr4a1 is closely related to TGF-β, and it has been reported that Nr4a1 induces cell differentiation [21, 22]. Therefore, we focused on the role of Nr4a1 in the differentiation of TDSCs regulated by 532 nm laser irradiation.

The expression of Nr4a1 was increased in injured tendons of the rat model after 532 nm laser intervention.

H&E staining was used to observe the repair of tendon tissue in the two groups (Fig. 6a). At 7 d, the damaged tendon fibers in the control group were arranged in a disordered manner, with irregular cell morphology and more “vacuole-type” structures. At 14 d, in the 532 nm laser group, the structure of the Achilles tendon was denser, the arrangement was orderly, and the infiltration of inflammatory cells was lower. The results showed that the repair effect in the 532 nm laser group was better than that of the control group.

To verify whether Nr4a1 was expressed in tendon tissues after 532 nm laser intervention, the expression of Nr4a1 in Achilles tendon tissue was analyzed by immunohistochemical staining. The results revealed that the expression of Nr4a1 in Achilles tendon tissue was significantly increased in the laser-treated group compared with the control group (Fig. 6b and 6c).

Nr4a1 inhibited the expression of Scx and Tnmd to regulate the differentiation of TDSCs induced by 532 nm laser irradiation.

To preliminarily explore the role of Nr4a1 in the differentiation of TDSCs induced by 532 nm laser irradiation, RT-PCR was used to analyze the expression of the Nr4a1 gene in TDSCs of the 532 nm laser group and the expression changes of Scx and Tnmd in TDSCs of the transfected Nr4a1 siRNA$^+$ 532 nm laser group. The results showed that Nr4a1 expression after 532 nm laser irradiation of TDSCs was significantly increased compared with the control group (2.74-Fold, $P < 0.01$) (Fig. 7a). The expression levels of *Scx* and *Tnmd* genes in the Nr4a1 siRNA+532 nm laser group were significantly down-regulated compared with the 532 nm laser group ($P < 0.05$) (Fig. 7b). The expression levels of the proteins Scx and Tnmd related to tendon differentiation in TDSCs in the 532 nm laser group were significantly increased compared with the control group ($P < 0.05$), while the expression levels of proteins Scx and Tnmd in the Nr4a1 siRNA$^+$ 532 nm laser group were significantly decreased compared with the 532 nm laser group ($P < 0.05$) (Fig. 7c and 7d). These results show that inhibiting the expression of Nr4a1 also blocked the expression of Scx and Tnmd.

Discussion

Over recent years, low-level laser therapy (LLLT) has achieved good efficacy in inhibiting inflammation, relieving pain, and promoting injury repair. Some researchers used an 808 nm laser of 6.38 J/cm^2 to irradiate the wound in a rat injury model, and the results showed that the wound surface contraction rate of the 808 nm laser group was faster than that of the control group at 2 weeks after injury, while the average wound healing rate was significantly higher [23]. The role of LLLT in the repair of tendon injury has attracted increasing attention. In our previous study, we used a 532 nm laser combined with the photosensitizing agent Rose Bengal (RB) to treat an Achilles tendon injury in rats and observed that this treatment significantly promoted the repair of the injured Achilles tendon. Further studies revealed that the tendon cells treated with the 532 nm laser exhibited sustained and low release of reactive oxygen species (ROS), which could activate the RhoA/NF-B pathway, promote the proliferation and migration of tendon cells, and accelerate tendon healing [15, 16]. Therefore, in this study, we wanted to investigate whether a 532 nm laser promoted the repair of injured tendon by regulating the proliferation and differentiation of TDSCs.

Previous studies have confirmed that LLLT promoted the proliferation of vascular endothelial cells, osteoblasts, and other cell types. Some researchers believe that the main reason why LLLT promotes cell proliferation is that the colored groups in mitochondria absorb and convert the light energy from LLLT irradiation into chemical energy, which is stored and utilized in the form of ATP, so as to enhance cell proliferation and activation [24]. Altan *et al.* irradiated the damaged upper incisors of mice with a laser of 15 J/cm^2 at 830 nm wavelengths. After 1 week, they found increased neovascularization, significant proliferation of osteoblasts and osteoclasts, and accelerated bone reconstruction [25]. The regulation and differentiation induced by LLLT is closely related to the energy density and wavelength of the laser [26]. In this experiment, we investigated the energy density and found that the proliferation capacity of TDSCs was significantly enhanced when the energy density exceeded 6 J/cm^2. At the same time, we found no significant difference in proliferation capacity between the groups treated with energy densities of 15

J/cm^2 and 24 J/cm^2. Therefore, we chose 15 J/cm^2 as the appropriate energy density for subsequent studies.

Scx and Tnmd are not only important transcription factors expressed in TDSCs during tendon differentiation but also key genes related to the formation and development of tendons [27]. Nicholas *et al.* pointed out that when gene knockout technology was used to construct Scx-deficient mice, their tendon tissues were naturally deficient due to the decrease of tendon matrix and disordered fiber arrangement, indicating the importance of Scx in the process of tendon formation [28]. TDSCs spontaneously express Scx and Tnmd. When TDSCs differentiate into adipocytes or chondrocytes, the expression of Scx and Tnmd are significantly decreased, while the expression of Scx and Tnmd are often increased during the differentiation of TDSCs into tendons and ligaments, thus indicating that Scx and Tnmd have a certain specific correlation with the differentiation of tendons [29]. Therefore, we used Scx and Tnmd as two observational indicators to judge the differentiation of TDSCs. RT-RCR and western blot detection showed that both the gene and protein levels of Scx and Tnmd of TDSCs at different phase points after 532 nm laser irradiation were significantly higher than those of the control group ($P < 0.01$), suggesting that a 532 nm laser could regulate the tendon differentiation of TDSCs.

Orphan nuclear receptor NR4A1, a member of the early response gene family, also known as Nur77 or TR3, is widely expressed in a variety of tissues, including skin, muscle, and blood [30]. It is rapidly expressed under chemical and physical stimulation and specifically combines with the regulatory region of the target gene to exert its role in regulating gene transcription, thus participating in cell survival and apoptosis, energy metabolism, inflammatory response regulation, angiogenesis and remodeling, and other cellular biological behaviors [21, 31]. Some studies have shown that Nr4a1 inhibited apoptosis by reducing the activity of caspase 3/caspase 8 [32]. Moreover, it regulates the expression of cell cycle genes and promotes cell proliferation and differentiation [33]. Some experiments found that in Nr4a1-deficient mice, the apoptosis of bone-marrow-derived monocytes was accelerated, and their differentiation was inhibited [34]. However, the mechanism via which Nr4a1 regulates cell differentiation is still unclear. By comparing the transcription levels of Nr4a1-deficient mice with those of normal mice, it was found that Nr4a1 inhibited the differentiation of T cells into regulatory T cells by activating the mTOR/Akt pathway. Thus, Nr4a1 has an important role in regulating cell differentiation [35].

In this study, we found that Nr4a1 expression was significantly increased in TDSCs after 532 nm laser irradiation, through RNA sequencing technology (RNA-seq) and GO and KEGG analysis. Moreover, Nr4a1 was closely related to the skeletal muscle development pathway, and we believe that Nr4a1 has an important role in this process. We used Nr4a1 siRNA to inhibit the expression of Nr4a1, which targeted Nr4a1 by interfering with Nr4a1 gene expression via mRNA degradation after transcription, resulting in translation blockage. Our results indicated that Nr4a1 siRNA inhibited the expression of the tenogenic differentiation-related genes *Scx* and *Tnmd* in TDSCs.

Our KEGG pathway analysis suggested that highly-enriched TGF pathways were activated during this process. There is a negative feedback loop between Nr4a1 and TGF-β which jointly regulate fibrosis in

tissues [22]. Some studies have pointed out that the TGF-β signaling pathway was closely related to Scx, TGF-β regulates the expression of Scx and Tnmd by activating Smad 2/3 and regulating the downstream Sox9 [36]. From the perspective of embryonal development, TGF-β stimulates the differentiation of mesoderm cells towards the tendon-forming direction and inhibits chondrogenesis at the same time [37]. Considering the above, it is reasonable to speculate that Nr4a1 regulates the tenogenic differentiation factors Scx and Tnmd of TDSCs by regulating the TGF-β signaling pathway. Further experiments are needed to verify this hypothesis.

Conclusions

In summary, we successfully isolated and identified tendon-derived stem cells (TDSCs) from SD rats in this study. After finding the ideal 532 nm laser energy density, the effect of a 532 nm laser on the proliferation and differentiation of TDSCs was verified. Then, bioinformatics analysis revealed that 532 nm laser-treated TDSCs exhibited high Nr4a1 expression. At the same time, by transfecting TDSCs with an Nr4a1 siRNA plasmid, we verified that Nr4a1 acted during 532 nm laser irradiation to induce TDSCs to differentiate into tendon and plays a role in the process. Meanwhile inhibiting the Nr4a1 expression of TDSCs obviously decreased the expression of the tendon differentiation markers Scx and Tnmd at the gene and protein levels in the 532 nm laser treatment group. Therefore, we speculated that 532 nm laser irradiation of TDSCs activated the early response gene Nr4a1 to regulate the generation of tendon differentiation markers such as Scx and Tnmd, promoting the differentiation of TDSCs into tendon cells and thus promoting the repair of injured tendon. However, the specific intrinsic molecular mechanisms still need to be verified by further experiments.

Abbreviations

AAALAC: Association for Assessment and Accreditation of Laboratory Animal Care International; AKT: AKT serine/threonine kinase 1; AT: Achilles tendons; BMSCs: Bone marrow stem cells; Btg2: BTG anti-proliferation factor 2; CTG: Cell Titer-Glo; *Dcn*: Decorin; DMEM: Dulbecco's modified eagle medium; EDTA: ethylenediaminetetraacetic acid; EGR: Early growth response1; FITC: Fluorescein isothiocyanate; GAPDH: Glyceraldehyde-3-phosphate dehydrogenase; GO: Gene ontology; H&E: Hematoxylin and eosin; HG-DMEM: High glucose DMEM; IACUC: Institutional Animal Care and Use Committee; KEGG: Kyoto Encyclopedia of Genes and Genomes; LLLT: Low-level laser therapy; *Mkx*: Mohawk homeobox; MSCs: Mesenchymal stem cells; NF-κB: Nuclear factor kappa B; Nr4a1: Nuclear receptor subfamily 4 group A member 1; OD: Optical density; PBS: Phosphate buffered saline; PFA: Paraformaldehyde; *PPARγ*: Peroxisome proliferator activated receptor gamma; PTB: Photochemical tissue bonding; RhoA: Ras homolog family member A; RB: Rose Bengal; RNA-seq: RNA sequencing; ROS: reactive oxygen species; RT-PCR: Reverse Transcription-Polymerase Chain Reaction; *Runx2*: RUNX family transcription factor 2; RT: Room temperature; *Scx*: Scleraxis; SD: **S**tandard deviation; SD rat: Sprague-Dawley rat; SDS: **S**odium dodecyl sulfate; SDS-PAGE: SDS polyacrylamide gel electrophoresis; *Sox9*: SRY-box transcription factor 9; TDSC: Tendon-derived stem cells; TGF-β: **T**ransforming growth factor-β; *TNMD*: Tenomodulin

Declarations

Acknowledgments

Not applicable.

Authors' contributions

TN, YHD and ML conceived and designed the experiments; ML and YMZ performed the experiments; QP and YHD contributed materials; QP, ML and YHD contributed data analysis; ML, YMZ wrote the manuscript and TN revised it. All authors read and approved the final manuscript.

Funding

This work was supported by Shanghai Municipal Key clinical specialty(shslczdzk00901), Shanghai Ninth People's Hospital cross funding (JYJC202101), and Shanghai Sailing Program (21YF1422800).

Availability of data and materials

The data and materials used in the current study are all available from the corresponding author upon reasonable request.

Ethics approval and consent to participate

All animal studies (including the rat euthanasia procedure) were carried out in compliance with the regulations and guidelines of Shanghai Jiao Tong University institutional animal care and conducted according to the AAALAC and the IACUC guidelines.

Consent for publication

Not applicable.

Competing interests

The authors declare that there are no competing interests.

Author details

[1]Department of Plastic and Reconstructive Surgery Shanghai Ninth People's Hospital, School of Medicine, Shanghai Jiao Tong University, Shanghai 200011, China.

[2]Department of General Surgery, Shanghai Ninth People's Hospital, School of Medicine, Shanghai Jiao Tong University, Shanghai 200011, China.

[3]Department of Orthopedic Surgery, Shanghai Sixth People's Hospital, Shanghai Jiao Tong University, Shanghai 200233, China.

References

1. Hodgins JL, Trofa DP, Donohue S, Littlefield M, Schuk M, Ahmad CS. Forearm Flexor Injuries Among Major League Baseball Players: Epidemiology, Performance, and Associated Injuries. Am J Sports Med. 2018;46(9):2154–60. https://doi.org/10.1177/0363546518778252.
2. Lian ц≤, Scott A, Engebretsen L, Bahr R, Duronio V, Khan K. Excessive apoptosis in patellar tendinopathy in athletes. Am J Sports Med. 2007;35(4):605–11. https://doi.org/10.1177/0363546506295702.
3. Arnoczky SP, Lavagnino M, Egerbacher M. The mechanobiological aetiopathogenesis of tendinopathy: is it the over-stimulation or the under-stimulation of tendon cells? Int J Exp Pathol. 2007;88(4):217–26. https://doi.org/10.1111/j.1365-2613.2007.00548.x.
4. Im GI. Tissue Engineering in Osteoarthritis: Current Status and Prospect of Mesenchymal Stem Cell Therapy. BioDrugs: clinical immunotherapeutics, biopharmaceuticals and gene therapy. 2018;32(3):183-192. https://doi.org/10.1007/s40259-018-0276-3.
5. Veronesi F, Della Bella E, Torricelli P, Pagani S, Fini M. Effect of adipose-derived mesenchymal stromal cells on tendon healing in aging and estrogen deficiency: an in vitro co-culture model. Cytotherapy. 2015;17(11):1536–44. https://doi.org/10.1016/j.jcyt.2015.07.007.
6. Schneider M, Angele P, Jцrvinen TAH, Docheva D. Rescue plan for Achilles: Therapeutics steering the fate and functions of stem cells in tendon wound healing. Adv Drug Deliv Rev. 2018;129:352–75. https://doi.org/10.1016/j.addr.2017.12.016.
7. Lui PPY, Wong CM. Biology of Tendon Stem Cells and Tendon in Aging. Frontiers in genetics. 2019;10:1338. https://doi.org/10.3389/fgene.2019.01338.
8. Bian X, Liu T, Zhou M, He G, Ma Y, Shi Y, et al. Absence of estrogen receptor beta leads to abnormal adipogenesis during early tendon healing by an up-regulation of PPARнЁ signalling. J Cell Mol Med. 2019;23(11):7406–16. https://doi.org/10.1111/jcmm.14604.
9. Lui PP, Wong OT, Lee YW. Transplantation of tendon-derived stem cells pre-treated with connective tissue growth factor and ascorbic acid in vitro promoted better tendon repair in a patellar tendon window injury rat model. Cytotherapy. 2016;18(1):99–112. https://doi.org/10.1016/j.jcyt.2015.10.005.
10. Bensadoun RJ. Photobiomodulation or low-level laser therapy in the management of cancer therapy-induced mucositis, dermatitis and lymphedema. Current opinion in oncology. 2018;30(4):226–32. https://doi.org/10.1097/cco.0000000000000452.
11. Avci P, Gupta A, Sadasivam M, Vecchio D, Pam Z, Pam N, et al. Low-level laser (light) therapy (LLLT) in skin: stimulating, healing, restoring. Semin Cutan Med Surg. 2013;32(1):41–52.
12. Kennedy J, Verne S, Griffith R, Falto-Aizpurua L, Nouri K. Non-invasive subcutaneous fat reduction: a review. Journal of the European Academy of Dermatology Venereology: JEADV. 2015;29(9):1679–88. https://doi.org/10.1111/jdv.12994.

13. Tani A, Chellini F, Giannelli M, Nosi D, Zecchi-Orlandini S, Sassoli C. Red (635 nm), Near-Infrared (808 nm) and Violet-Blue (405 nm) Photobiomodulation Potentiality on Human Osteoblasts and Mesenchymal Stromal Cells: A Morphological and Molecular In Vitro Study. Int J Mol Sci. 2018;19(7). https://doi.org/10.3390/ijms19071946.
14. Zare F, Moradi A, Fallahnezhad S, Ghoreishi SK, Amini A, Chien S, et al. Photobiomodulation with 630 plus 810Бnm wavelengths induce more in vitro cell viability of human adipose stem cells than human bone marrow-derived stem cells. J Photochem Photobiol B. 2019;201:111658. https://doi.org/10.1016/j.jphotobiol.2019.111658.
15. Ni T, Senthil-Kumar P, Dubbin K, Aznar-Cervantes SD, Datta N, Randolph MA, et al. A photoactivated nanofiber graft material for augmented Achilles tendon repair. Lasers Surg Med. 2012;44(8):645–52. https://doi.org/10.1002/lsm.22066.
16. Yao ZC, Wang x, Zhang W, Liu YS, Ni T. Photochemical tissue bonding promotes the proliferation and migration of injured tenocytes through ROS/RhoA/NF-kappaB/Dynamin 2 signaling pathway. J Cell Physiol. 2018;233(10):7047–56. https://doi.org/10.1002/jcp.26628.
17. Yang G, Rothrauff BB, Tuan RS. Tendon and ligament regeneration and repair: clinical relevance and developmental paradigm. Birth defects research. Part C, Embryo today: reviews. 2013;99(3):203–222. https://doi.org/10.1002/bdrc.21041.
18. Voleti PB, Buckley MR, Soslowsky LJ. Tendon healing: repair and regeneration. Annu Rev Biomed Eng. 2012;14:47–71. https://doi.org/10.1146/annurev-bioeng-071811-150122.
19. Akamatsu FE, Saleh SO, Teodoro WR, da Silva AQ, Martinez CAR, Duarte RJ, et al. Experimental model of Achilles tendon injury in rats. Acta Cir Bras. 2014;29(7):417–22. https://doi.org/10.1590/s0102-86502014000700002.
20. Lui PPY, Chan KM. Tendon-derived stem cells (TDSCs): from basic science to potential roles in tendon pathology and tissue engineering applications. Stem Cell Rev Rep. 2011;7(4):883–97. https://doi.org/10.1007/s12015-011-9276-0.
21. Qin DD, Yang YF, Pu ZQ, Liu D, Yu C, Gao P, et al. NR4A1 retards adipocyte differentiation or maturation via enhancing GATA2 and p53 expression. J Cell Mol Med. 2018;22(10):4709–20. https://doi.org/10.1111/jcmm.13715.
22. Palumbo-Zerr K, Zerr P, Distler A, Fliehr J, Mancuso R, Huang JG, et al. Orphan nuclear receptor NR4A1 regulates transforming growth factor-beta signaling and fibrosis. Nat Med. 2015;21(2):150–8. https://doi.org/10.1038/nm.3777.
23. Tabakoglu HO, Sani MM, Uba AI, Abdullahi UA. Assessment of circular wound healing in rats after exposure to 808-nm laser pulses during specific healing phases. Lasers Surg Med. 2016;48(4):409–15. https://doi.org/10.1002/lsm.22462.
24. Aihara N, Yamaguchi M, Kasai K. Low-energy irradiation stimulates formation of osteoclast-like cells via RANK expression in vitro. Lasers Med Sci. 2006;21(1):24–33. https://doi.org/10.1007/s10103-005-0368-4.

25. Altan BA, Sokucu O, Ozkut MM, Inan S. Metrical and histological investigation of the effects of low-level laser therapy on orthodontic tooth movement. Lasers Med Sci. 2012;27(1):131–40. https://doi.org/10.1007/s10103-010-0853-2.
26. Kuffler DP. Photobiomodulation in promoting wound healing: a review. Regenerative medicine. 2016;11(1):107–22. https://doi.org/10.2217/rme.15.82.
27. Liu C, Luo JW, Zhang KK, Lin LX, Liang T, Luo ZP, et al. Tendon-Derived Stem Cell Differentiation in the Degenerative Tendon Microenvironment. Stem cells international. 2018;2018:2613821. https://doi.org/10.1155/2018/2613821.
28. Murchison ND, Price BA, Conner DA, Keene DR, Olson EN, Tabin CJ, et al. Regulation of tendon differentiation by scleraxis distinguishes force-transmitting tendons from muscle-anchoring tendons. Development. 2007;134(14):2697–708. https://doi.org/10.1242/dev.001933.
29. Liu H, Zhu S, Zhang C, Lu P, Hu J, Yin Z, et al. Crucial transcription factors in tendon development and differentiation: their potential for tendon regeneration. Cell tissue research. 2014;356(2):287–98. https://doi.org/10.1007/s00441-014-1834-8.
30. Wu L, Amarachintha S, Xu J, Oley F, Du W. Mesenchymal COX2-PG secretome engages NR4A-WNT signalling axis in haematopoietic progenitors to suppress anti-leukaemia immunity. Br J Haematol. 2018;183(3):445–56. https://doi.org/10.1111/bjh.15548.
31. Freire PR, Conneely OM. NR4A1 and NR4A3 restrict HSC proliferation via reciprocal regulation of C/EBPalpha and inflammatory signaling. Blood. 2018;131(10):1081–93. https://doi.org/10.1182/blood-2017-07-795757.
32. Yang YF, Xie FY, Qin DD, Zong C, Han F, Pu ZQ, et al. The orphan nuclear receptor NR4A1 attenuates oxidative stress-induced beta cells apoptosis via up-regulation of glutathione peroxidase 1. Life Sci. 2018;203:225–32. https://doi.org/10.1016/j.lfs.2018.04.027.
33. Shi X, Ye H, Yao X, Gao Y. The involvement and possible mechanism of NR4A1 in chondrocyte apoptosis during osteoarthritis. American journal of translational research. 2017;9(2):746–54.
34. Hu C, Zhang Y, Tang K, Luo Y, Liu Y, Chen W. Downregulation of CITED2 contributes to TGFн-mediated senescence of tendon-derived stem cells. Cell tissue research. 2017;368(1):93–104. https://doi.org/10.1007/s00441-016-2552-1.
35. Chen L, Jiang C, Tiwari SR, Shrestha A, Xu P, Liang W, et al. TGIF1 Gene Silencing in Tendon-Derived Stem Cells Improves the Tendon-to-Bone Insertion Site Regeneration. Cellular physiology and biochemistry: international journal of experimental cellular physiology, biochemistry, and pharmacology. 2015;37(6):2101–2114. https://doi.org/10.1159/000438568.
36. Maeda T, Sakabe T, Sunaga A, Sakai K, Rivera AL, Keene DR, et al. Conversion of mechanical force into TGF-н-mediated biochemical signals. Current biology: CB. 2011;21(11):933–41. https://doi.org/10.1016/j.cub.2011.04.007.
37. Igarashi Y, Chosa N, Sawada S, Kondo H, Yaegashi T, Ishisaki A. VEGF-C and TGF-н reciprocally regulate mesenchymal stem cell commitment to differentiation into lymphatic endothelial or

osteoblastic phenotypes. Int J Mol Med. 2016;37(4):1005–13. https://doi.org/10.3892/ijmm.2016.2502.

Tables

Table 1 Primer sequences (5'-3') used in real time RT-PCR.

Gene	Primer sequences
Scx	Forward AACACGGCCTTCACTGCGCTG
	Reverse CAGTAGCACGTTGCCCAGGTG
Tnmd	Forward CCAGACAAGCAAGCGAGGA
	Reverse AACTTCCTATTAGACTCTCC
Mkx	Forward AGTGGCTTTACAAGCACCGT
	Reverse ACACTGAGCCGCTCGGCGTT
Dcn	Forward TTGCAGGGAATGAAGGGTCT
	Reverse TGTGGGTGAATTTGCCAATA
GADPH	Forward ACAGCAACAGGGTGGTGGAC
	Reverse TTTGAGGGTACAGCGAACTT
PPARγ	Forward CGGCGATCTTGACAGGAAAG
	Reverse GCTTCCACGGATCGAAACTG
SOX9	Forward AGAGCGTTGCTCGGAACTGT
	Reverse TCCTGGACCGAAACTGGTAAA
RUNX2	Forward CCGATGGGACCGTGGTT
	Reverse CAGCAGAGGCATTTCGTAGCT
Nr4a1	Forward ATGCGATTCTGCAGCTCTTCC
	Reverse GGGTGGTATTGTCGTAGTAGAAGG

Figures

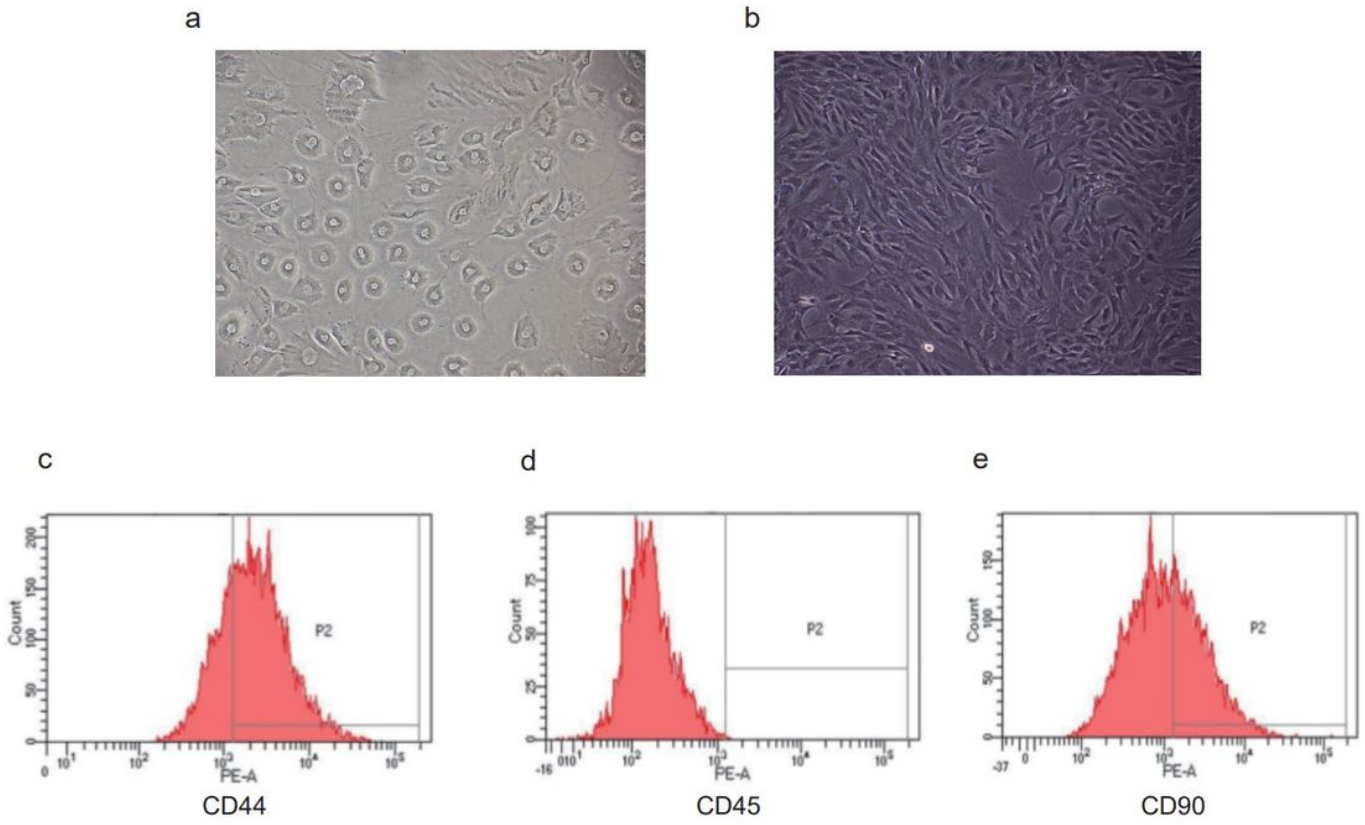

Figure 1

(a.b) Morphological characteristics of TDSCs and identification by flow cytometry. (c-e) Morphological characteristics of TDSCs from generation 0 and 3. Identification of TDSCs by flow cytometry for CD44, CD90 (positive markers), and CD45 (negative marker)

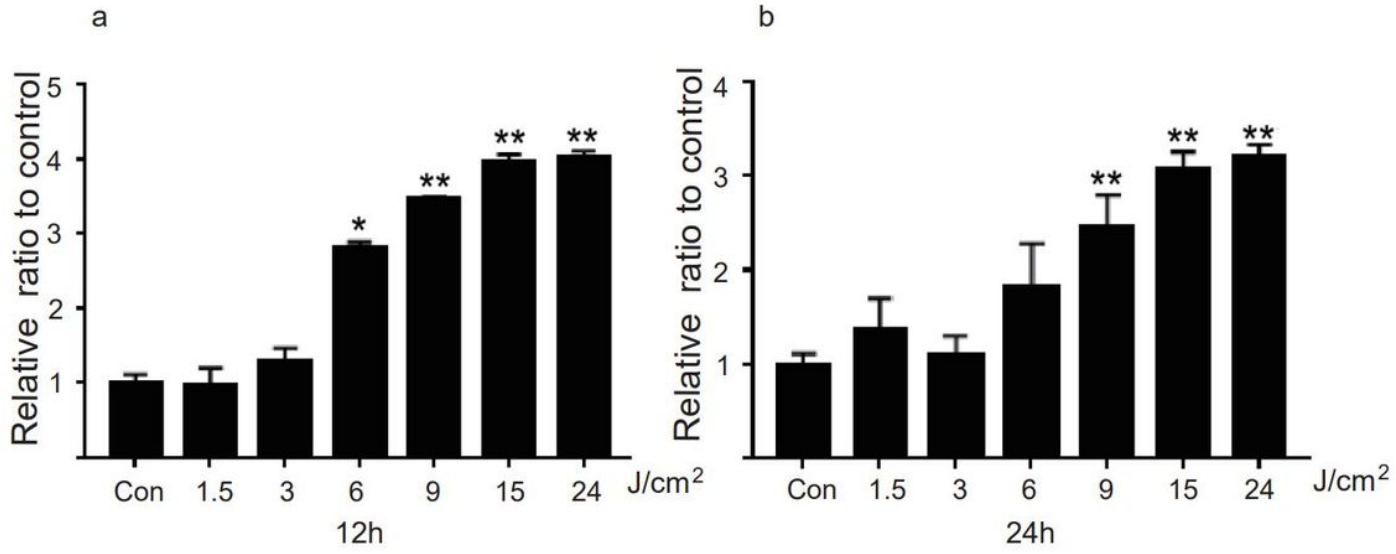

Figure 2

Effects of 532 nm laser with different energy density on cell viability of TDSCs. (a) Cell viability of TDSCs was detected by CTG after 24h of laser intervention with 532 nm (n=6, *P < 0.05, **P < 0.01). (b) Cell viability of TDSCs was detected by CTG after 48h of laser intervention with 532 nm (n=6, *P < 0.05, **P < 0.01).

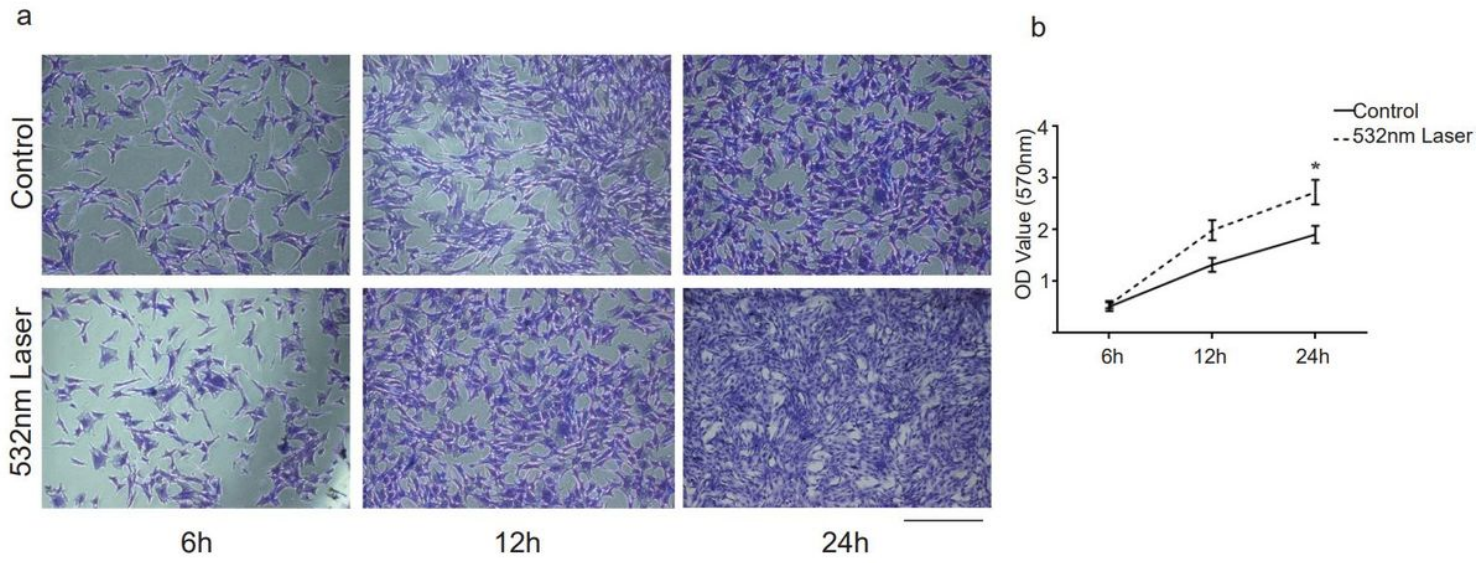

Figure 3

Effects of 532 nm laser on the proliferation of TDSCs. (a) The TDSCs of the control group and the 532 nm laser group were compared at 6h, 12h, and 24h by crystal violet staining. (b) The OD value of each group was detected, and the cell proliferation was quantitatively compared (n=6, *P < 0.05).

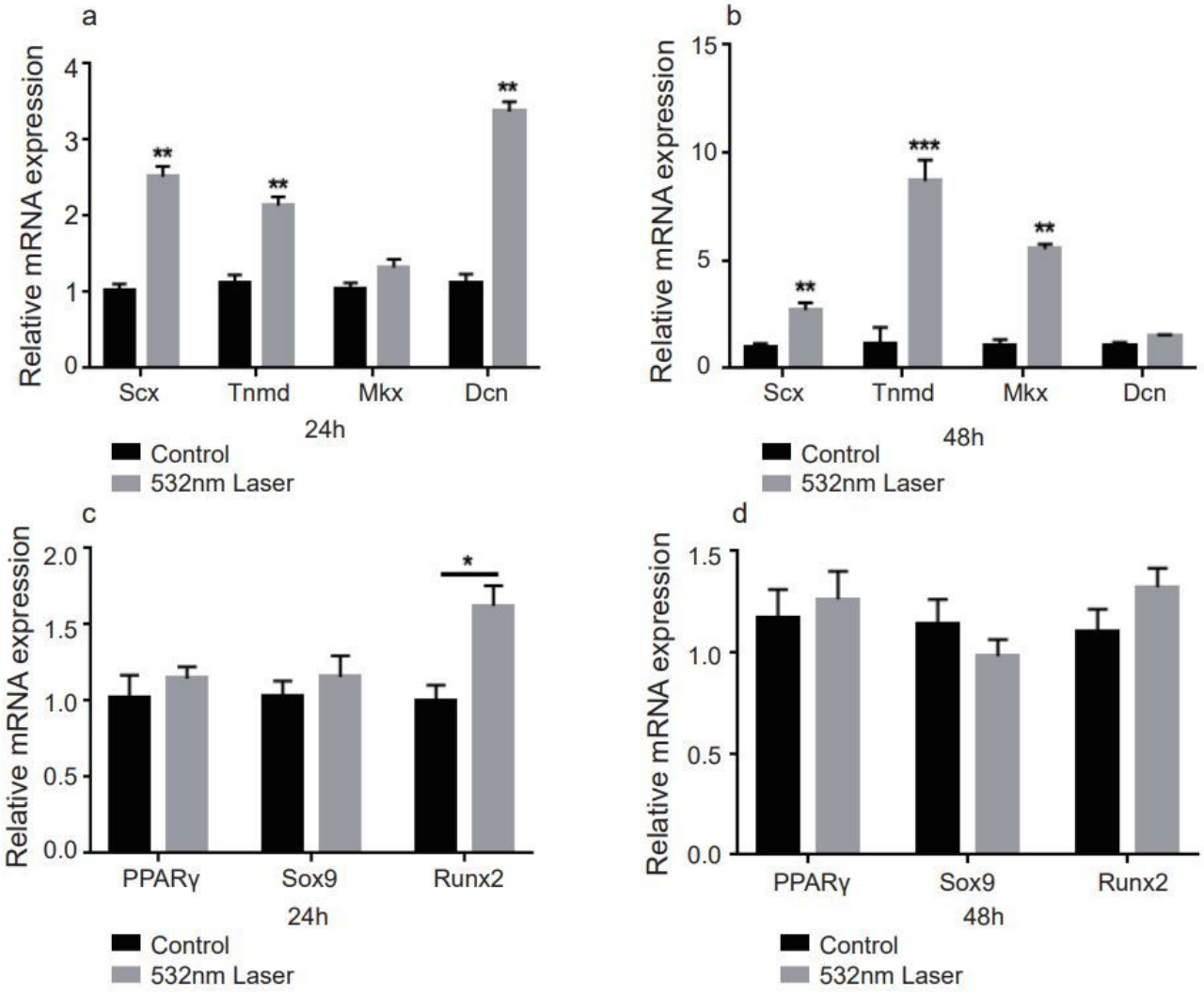

Figure 4

Effects of 532 nm laser on differentiation of TDSCs. (a) The expression of tenogenic differentiation markers of TDSCs after 24h of TDSCs intervention with 532 nm laser (n=6, **P<0.01). (b) The expression of tenogenic differentiation markers of TDSCs after 24h of TDSCs intervention with 532 nm laser (n=6, **P<0.01 ***<0.001). (c) The expression of adipogenic differentiation, chondrogenic differentiation, and osteogenic differentiation markers of TDSCs after 24h of TDSCs intervention by 532 nm laser (n=6, *P<0.05). (d) The expression of adipogenic differentiation, chondrogenic differentiation, and osteogenic differentiation markers of TDSCs after 48h of TDSCs intervention by 532 nm laser.

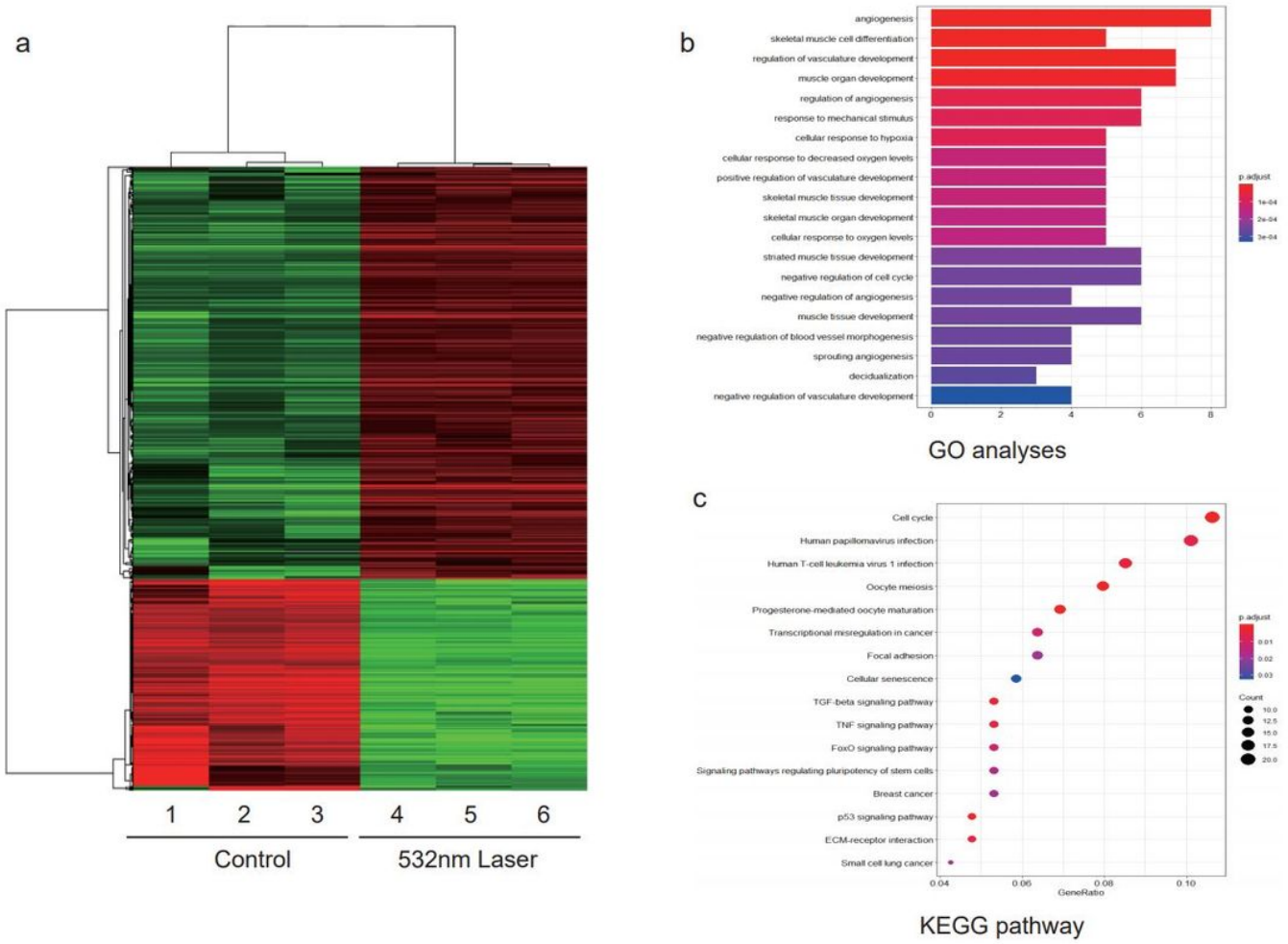

Figure 5

Gene expression profile of Rat Achilles tendon tissue. (a) Results of gene chip microarray in the control group and 532 nm laser group. (b) The top 20 biological processes enriched in the up-regulated genes by GO analysis of up-regulated genes. (c) The top 20 canonical pathways enriched in the up-regulated genes by KEGG pathway analysis.

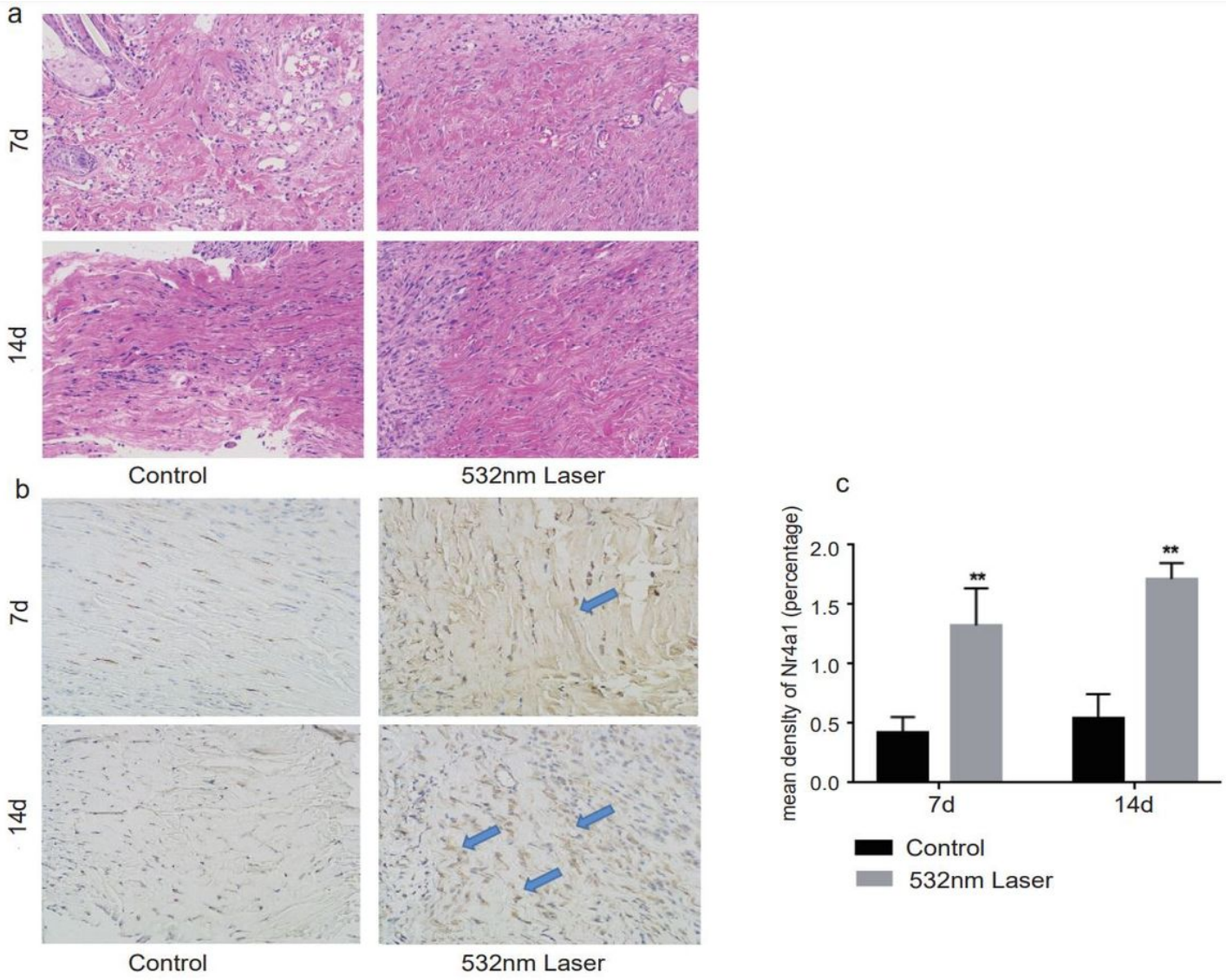

Figure 6

The expression of Nr4a1 in Achilles tendon tissue of rats. (a) The repair of the injured Achilles tendon in the control group and 532 nm laser group was observed by HE staining, x200 (b) The expression of Nr4a1 was detected by immunohistochemistry in human samples. x200. (c) A significant difference in Nr4a1 expression level between control group and the 532 nm laser group (n=3, **P<0.01).

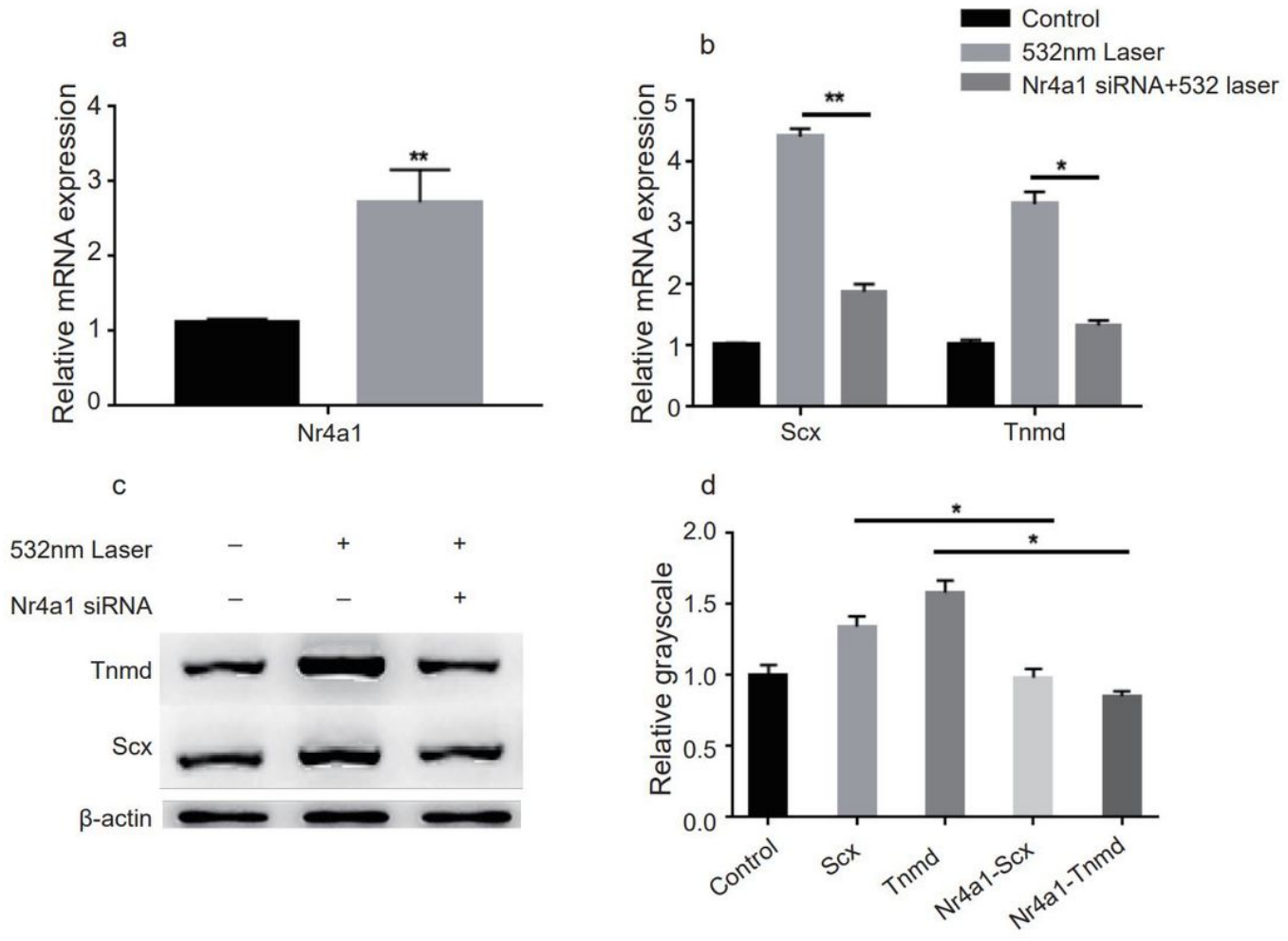

Figure 7

Nr4a1 inhibition by siRNA influences the expression of tenogenic differentiation markers of TDSCs. (a) Nr4a1 was highly expressed in TDSCs after 532 nm laser intervention (n=6, **P<0.01). (b) The RT-PCR analysis of the mRNA levels of Scx, Tnmd expression in TDSCs (n=6, *P<0.05, **P<0.01). (c) Western blot analysis of the protein levels of expression Scx, Tnmd expression in TDSCs. (d) The grayscale value of the strip was detected, and the expressions of Scx and Tnmd were quantitatively analyzed (n=3, *P<0.05).